

# Optimizing the second hyperpolarizability with minimally-parametrized potentials

C. J. Burke and T. J. Atherton

*Department of Physics and Astronomy, Center for Nanoscopic Physics,  
Tufts University, 4 Colby Street, Medford, MA. 02155*

J. Lesniewski

*Department of Physics, University of Illinois at Chicago, 845 W. Taylor St., Chicago, IL 60607-7059*

R. G. Petschek

*Department of Physics, Case Western Reserve University,  
10900 Euclid Avenue, Cleveland, Ohio, USA 44106*

The dimensionless zero-frequency intrinsic second hyperpolarizability  $\gamma_{int} = \gamma/4E_{10}^{-5}m^{-2}(e\hbar)^4$  was optimized for a single electron in a 1D well by adjusting the shape of the potential. Optimized potentials were found to have hyperpolarizabilities in the range  $-0.15 \lesssim \gamma_{int} \lesssim 0.60$ ; potentials optimizing gamma were arbitrarily close to the lower bound and were within  $\sim 0.5\%$  of the upper bound. All optimal potentials possess parity symmetry. Analysis of the Hessian of  $\gamma_{int}$  around the maximum reveals that effectively only a single parameter, one of those chosen in the piecewise linear representation adopted, is important to obtaining an extremum. Prospects for designing new chromophores based on the design principle here elucidated are discussed.

## I. INTRODUCTION

Developing materials with high electronic nonlinear susceptibilities is of fundamental importance for a wide variety of applications such as optical solitons, phase conjugate mirrors and optical self-modulation [1, 2]. These susceptibilities are defined by considering a material in the presence of an electric field  $E$  and expanding the induced polarization in a Maclaurin series,

$$P = \alpha E + \beta EE + \gamma EEE + O(E^4), \quad (1)$$

where the susceptibilities  $\alpha$ ,  $\beta$  and  $\gamma$  are generally frequency-dependent tensor quantities. Here, we consider the zero-frequency limit of these quantities in the non-resonant regime i.e. where all frequencies are much less than any resonant frequency of the electrons and motion of the nuclei is neglected. A remarkable result due to Kuzyk [3] is that quantum mechanics requires that the first and second hyperpolarizabilities  $\beta$  and  $\gamma$  are bounded: specifically,  $\gamma$  obeys the inequality,

$$-\left(\frac{e\hbar}{\sqrt{m}}\right)^4 \frac{N^2}{E_{10}^5} \leq \gamma \leq 4\left(\frac{e\hbar}{\sqrt{m}}\right)^4 \frac{N^2}{E_{10}^5} \equiv \gamma_0^{\max}, \quad (2)$$

where  $N$  is the number of electrons,  $E_{10}$  is the energy difference between the ground and first excited states and  $m$  is the electron mass. It is natural to define the intrinsic hyperpolarizability as a figure of merit to characterize the proximity of a given system to this limit,

$$\gamma_{int} = \gamma/\gamma_0^{\max} \quad (3)$$

and to ask: how to create materials that achieve optimal  $\gamma_{int}$ ? The discovery of the bounds (2) has motivated a number of experimental studies that have demonstrated that carefully tuning the electronic states and

geometry of chromophores can lead to higher second hyperpolarizabilities[4–7]. Generic design principles motivated by fundamental theory would therefore be desirable. Unfortunately, the procedure used to derive the bounds (2) cannot directly provide these; they were obtained by optimizing  $\gamma$  for a three-level ansatz with respect to the dipole matrix elements and energy level spacings  $E = E_{10}/E_{20}$  and *not* by constructing an explicit potential. Indeed, the assumptions behind the derivation have been questioned[8, 9] and the limits need not be achievable with a local potential; it has been speculated recently these may require exotic Hamiltonians[10].

Subsequent work, following approaches developed in earlier studies of  $\beta$ [11, 12], has attempted to address this in two ways: First, by identifying universal features of Hamiltonians near the fundamental limit by a Monte Carlo search[13] and, secondly, by numerically optimizing  $\gamma_{int}$  with respect to the shape of a local potential[10]. This latter work found potentials which have second hyperpolarizabilities in the range  $-0.15 \leq \gamma_{int} \leq 0.60$ , which represents an *apparent* bound that is more restrictive than the bound of (2). Moreover it was demonstrated that the optimized potentials spectra and dipole moments were broadly consistent with those identified in the earlier Monte Carlo study.

While these strategies provide useful goals for chemists attempting to design new nonlinear chromophores, they do not provide insight into which features of the potential are necessary to optimize  $\gamma_{int}$ , or how many free parameters should be necessary to achieve optimal or near optimal  $\gamma$ . In a previous paper[14], we developed a technique to examine the analogous question for  $\beta$ : by optimizing potentials described by increasing numbers of free parameters and examining the eigenvalues of the Hessian matrix at each maximum, we identified the combinations of parameters most important to the optimization. The analysis revealed that effectively only two parameters were

necessary to maximize  $\beta$ , and hence that a surprisingly broad range of potentials with high  $\beta$  exists around each maximum.

In this work, we apply the same technique to the problem of optimizing  $\gamma$ . At first sight, the problem appears to be more difficult than that for  $\beta$  since the expression for  $\gamma$  is much more complicated and the bounds for positive and negative  $\gamma$  are different. Remarkably, however, we will show that effectively only *one* parameter is necessary to optimize  $\gamma$  in either direction and, moreover, that in each case it is one of the parameters utilized in our representation of the potential. In this sense, we are able to suggest much more clearly a possible design strategy for materials with high  $\gamma$  than for  $\beta$  within the limitations of the model. At least within our representation of the potentials, we find that the potential that maximizes  $\gamma$  is rapidly varying, while for negative  $\gamma$ , as for  $\beta$ , quite generic, slowly varying potentials are adequate. The paper is organized as follows: in section II the calculations performed are described; the results are presented and discussed in section III; conclusions are drawn in section IV.

## II. MODEL

It is first necessary to generalize the method described our previous paper on optimizing the intrinsic first hyperpolarizability  $\beta_{int}$  [14]: in the present work,  $\gamma_{int}$  is to be optimized by adjusting the shape of a one-dimensional piecewise-linear potential. Such a potential with  $N + 1$  segments may be represented,

$$V(x) = \begin{cases} A_0x + B_0 & x < x_0 \\ A_nx + B_n & x_{n-1} < x < x_n, \quad n \in \{1, \dots, N-1\} \\ A_Nx + B_N & x > x_{N-1}, \end{cases} \quad (4)$$

with the positions  $x_n$  and slopes  $A_n$  as the adjustable parameters and where the  $B_n$  are chosen to enforce continuity. Because  $\gamma_{int}$  is invariant under trivial translations and rescalings of the potential, some of these parameters were fixed  $x_0 = 0$ ,  $B_0 = B_1 = 0$ , and  $A_1 = \pm 1$ . These choices, together with a change of origin and rescaling allow for any potential. Thus maximizing with these constraints allows faster optimization. Furthermore, the left- and right-most slopes are required to be negative and positive, respectively, ensuring only bound electron states. Finally, for technical reasons, having to do with the asymptotic behavior of the Airy functions introduced in eqn 7 below, it is difficult to allow the sign of any slope to change during an optimization. In consequence, we have chosen to restrict  $|A_i| > .005$ , and, as appropriate to do separate optimizations for each interesting sign of each slope.

A second representation for the potential was also considered where parity symmetry was specifically enforced. This was motivated by previous work[15] which identifies parity as important for optimizing  $\gamma_{int}$ , particularly for

the lower bound. The potentials with enforced  $\mathcal{P}$  symmetry were constructed on the half line  $x \geq 0$  with  $N$  segments,

$$V(x) = \begin{cases} A_nx + B_n & x_{n-1} < x < x_n, \quad n \in \{1, \dots, N-1\} \\ A_Nx + B_N & x > x_{N-1} \end{cases} \quad (5)$$

with  $x_0 = 0$  and requiring  $V(-x) = V(x)$ . Again  $x_n$  and  $A_n$  are adjustable parameters and  $x_0 = 0$ ,  $B_0 = B_1 = 0$  are fixed. The parameter  $A_1$  was set to either  $-1$  or  $+1$  to study the consequences of both cases.

For such a potential with a uniform applied electric field of strength  $\epsilon$ , the wavefunction obeys the Schrodinger equation in each segment,

$$\left[ -\frac{1}{2} \frac{d^2}{dx^2} + (A_n + \epsilon)x + B_n \right] \psi_n = E\psi_n, \quad (6)$$

in units such that  $e = 1$ ,  $\hbar = 1$ , and  $m_e = 1$ . The solution in each segment is written in terms of the well-known Airy functions,

$$\psi_n(x) = C_n \text{Ai} \left[ \frac{\sqrt[3]{2}(B_n - E + x(A_n + \epsilon))}{(A_n + \epsilon)^{2/3}} \right] + D_n \text{Bi} \left[ \frac{\sqrt[3]{2}(B_n - E + x(A_n + \epsilon))}{(A_n + \epsilon)^{2/3}} \right]. \quad (7)$$

To solve for the coefficients  $C_n$  and  $D_n$  the usual boundary conditions are imposed, i.e. that the wavefunction  $\psi(x)$  and its derivative  $\psi'(x)$  are continuous at the boundary between segments. Additionally, in the end segments, the wavefunction must vanish as  $x$  goes to  $\pm\infty$  fixing  $D_N = 0$ . There are a total of  $2N$  linear equations in the coefficients for the arbitrary case and  $4N - 2$  equations and coefficients for the  $\mathcal{P}$ -symmetric case, which can be written in matrix form

$$W \cdot u = 0 \quad (8)$$

where  $u$  is a vector comprised of the  $C_n$  and  $D_n$  coefficients and  $W$  is a matrix which depends on  $E$ ,  $\epsilon$  and the parameters  $A_n$  and  $x_n$ .

The allowed energy levels are found by numerically finding the roots of

$$\det W = 0 \quad (9)$$

with  $\epsilon = 0$ . It is readily possible, as previously done for  $\beta$ , to obtain from (8) an expression for the second hyperpolarizability,

$$\gamma \equiv \frac{1}{6} \left. \frac{d^4 E_0}{d\epsilon^4} \right|_{\epsilon=0}; \quad (10)$$

this is achieved by repeatedly differentiating the matrix  $W$  using the Jacobi formula,

$$\frac{d}{d\epsilon} \det W = \text{Tr} \left( \text{adj}W \cdot \frac{dW}{d\epsilon} \right), \quad (11)$$

where  $\text{adj}W$  is the adjugate of  $W$  (since  $W$  is singular), and applying the chain rule

$$\frac{dW}{d\epsilon} = \frac{\partial W}{\partial \epsilon} + \frac{\partial W}{\partial E} \frac{dE}{d\epsilon}. \quad (12)$$

Having performed similar calculations to those in [14], we arrive at the expression

$$\frac{d^4E}{d\epsilon^4} = - \frac{\text{Tr} \left[ \left( \frac{d^3}{d\epsilon^3} \text{adj}W \right) \cdot \frac{dW}{d\epsilon} + 3 \left( \frac{d^2}{d\epsilon^2} \text{adj}W \right) \cdot \frac{d^2W}{d\epsilon^2} + 3 \left( \frac{d}{d\epsilon} \text{adj}W \right) \cdot \frac{d^3W}{d\epsilon^3} + \text{adj}W \cdot W''' \right]}{\text{Tr} \left( \text{adj}W \cdot \frac{\partial W}{\partial E} \right)}, \quad (13)$$

where

$$W''' = \frac{d^4W}{d\epsilon^4} - \frac{\partial W}{\partial E} \frac{d^4E}{d\epsilon^4}. \quad (14)$$

From this,  $\gamma$  is readily obtained and the intrinsic second hyperpolarizability  $\gamma_{int} = \gamma/\gamma_0^{\text{max}}$  calculated for a given set of parameters.

The quantity  $\gamma_{int}$  was optimized numerically for both arbitrary and  $\mathcal{P}$ -symmetric potentials with varying numbers of segments using the `FindMaximum` function of *Mathematica* 8, an implementation of the Interior Point method for constrained optimization. Both maxima and minima of  $\gamma_{int}$  were obtained from a large number of randomly generated starting points, and also manually chosen starting points with large values for  $\gamma_{int}$ . Once an optimum  $\gamma_{int}$  was found, the extent to which each of the parameters was important to the extremum was characterized by calculating the Hessian matrix,

$$H_{ij} = \frac{\partial^2}{\partial P_i \partial P_j} \gamma_{int},$$

where the  $P_i$  are the parameters, and calculating its eigenvalues and eigenvectors. Since the Hessian matrix characterizes the local curvature of the objective function in the parameter space around the extremum, these quantities give the magnitudes and directions of the principal curvatures. As stressed in previous work[14] these curvatures implicitly depend on a measure implied by this equation that is peculiar to our numerical parameterization of the problem. More physically relevant measures can also be used to calculate eigenvalues. While these make quantitative changes in the eigenvalues and vectors, they do not make qualitative changes, and we give results for this “numerically natural” measure below.

### III. RESULTS AND DISCUSSION

Our optimized potentials, together with the ground and first excited state wavefunctions, are displayed in Fig. 1 for both arbitrary (eq. 4) and  $\mathcal{P}$ -symmetric (eq. 5) parametrizations. The associated parameter values are listed in Table I. The potentials and wavefunctions

are displayed on a transformed position and energy scale,

$$\bar{x} = (x - \langle x \rangle) / (E_1 - E_0)^{1/2} \\ \bar{V}(\bar{x}, \{P\}) = (V(\bar{x}, \{P\}) - E_0) / (E_1 - E_0) \quad (15)$$

such that the ground state energy is  $E_0 = 0$ , the difference between the ground and first excited state energy is  $E_1 - E_0 = 1$  and the position expectation value for the ground state is  $\langle x_0 \rangle = 0$ . This rescaling does not change  $\gamma_{int}$  and permits convenient comparison of the results of each optimization. To identify the relative importance of each of the parameters to the optimization, the results of the eigenanalysis of the Hessian matrix are also displayed for selected potentials in Fig. 1; the  $j$ -th eigenvalue of the Hessian,  $h^j$ , is listed alongside a plot of the variation in the potential  $\Delta V^j(x)$  in the direction of the associated eigenvector,

$$\Delta V^j(x) = \left. \frac{\partial \bar{V}(\bar{x}, \{P_i + \alpha v_i^j\})}{\partial \alpha} \right|_{\alpha=0}, \quad (16)$$

where  $v_i^j$  is the  $i^{\text{th}}$  component of the  $j$ -th eigenvector. Note that the values of  $V$  and  $x$  in the right hand side of (16) are renormalized as a function of  $\alpha$  using (15) so that the variations presented automatically preserve the properties  $\langle x_0 \rangle = 0$  and  $E_1 - E_0 = 1$ .

The first set of results displayed in Fig. 1(a) are optimized potentials with no enforced symmetry and specified by 3 or 5 free parameters. The optimized  $\gamma_{int}$  for both the lower and upper bounds of  $\gamma_{int}$  potentials fall somewhat below the apparent bounds observed in [13]. For the upper bound, the best results assuming all slopes except the first are positive are what appears to be a local maximum value of  $\gamma_{int} \simeq 0.43$  [Fig. 1(a)(ii)]. A similar value was also found in [10] for potentials with no constrained symmetry, but the potentials found here do not closely resemble those found in that work. The eigenvalues and eigenvectors displayed below the potential in [Fig. 1(a)(ii)] show that only two of the eigenvalues are significant in magnitude and are associated with the shape of the potential in the middle while the small eigenvalues are associated with the outer slopes. These results are reminiscent of those found for the first hyperpolarizability, where  $\beta_{int}$  was found to approach its maximum

Bound	Description	Ref.	$\gamma_{int}$	$A_0$	$A_2$	$A_3$	$x_1$	$x_2$
Upper	3 param. arb.	(a)(i)	0.43277	2.33932	0.10189	—	1.04960	—
	5 param. arb.	(a)(ii)	0.43602	4.28494	0.08829	0.37688	1.42131	3.95728
	2 param. $\mathcal{P}$	(b)(i)	0.58220	—	0.00550	—	0.57426	—
	3 param. $\mathcal{P}$	(b)(ii)	0.59707	—	0.00500	—	0.88533	7.95755
Lower	3 param. arb.	(a)(iii)	-0.11409	82.471	237.57	—	1.25227	—
	2 param. $\mathcal{P}$	(b)(iii)	-0.14996	—	31.6157	—	1.48005	—

Table I: List of parameters of optimized potentials

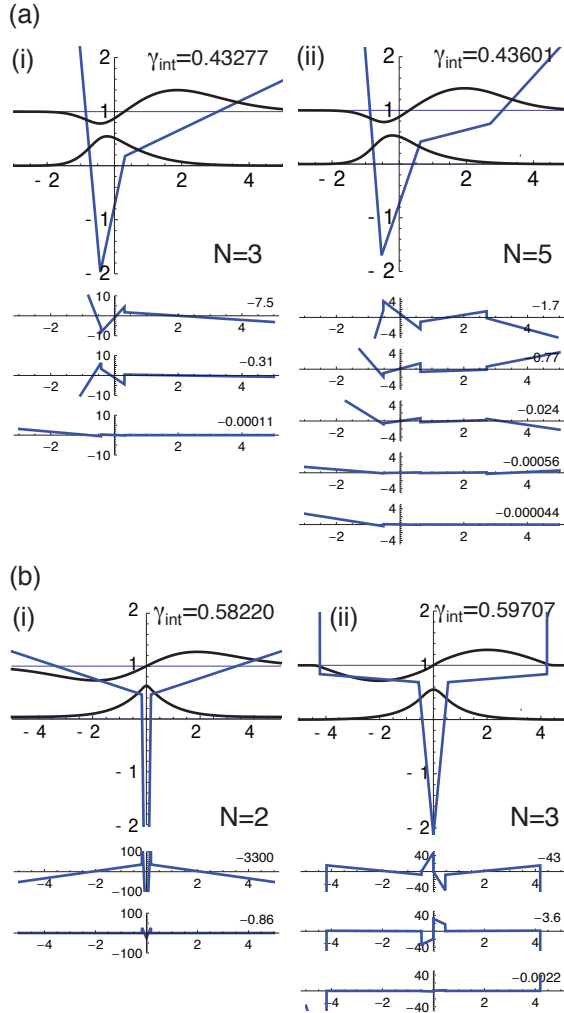


Figure 1: Optimized potentials for the *upper* bound of  $\gamma_{int}$  with (a) no enforced symmetry and (b)  $\mathcal{P}$ -symmetry. The energies of the ground and first excited state are indicated by horizontal lines; the corresponding wavefunctions are also displayed. The plots have been rescaled to facilitate comparison by ensuring  $E_1 - E_0 = 1$  and  $\langle x_0 \rangle = 0$  while preserving  $\gamma_{int}$ .

value for the same class of potentials with a similarly small number of parameters and analysis of the Hessian revealed that only effectively two parameters were important to the maximization. For the lower bound, the 3 parameter system [Fig. 2(a)] converges on a shape ap-

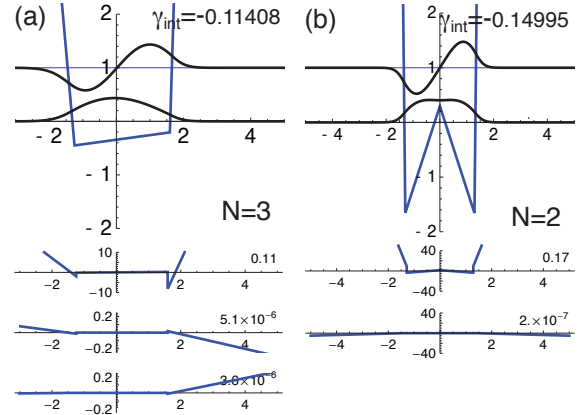


Figure 2: Optimized potentials for the *lower* bound of  $\gamma_{int}$  with (a) no enforced symmetry and (b)  $\mathcal{P}$ -symmetry.

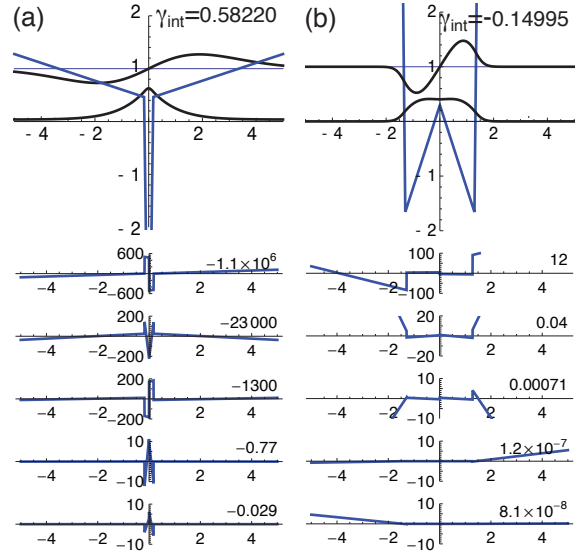


Figure 3: Five parameter potentials with no enforced symmetry optimized using two-parameter  $\mathcal{P}$ -symmetric optima as the starting point. (a) Upper and (b) lower bounds.

proaching a square well. The 5 parameter system also converges on a  $\mathcal{P}$ -symmetric potential and, because of this, further discussion of the lower bound is deferred to a subsequent paragraph.

A possible explanation for the fact that the optimized positive  $\gamma_{int}$  for arbitrary potentials in Fig. 1 falls short

of the bounds established in [3, 10, 13] is that the hyperpolarizability is sensitive only to some features of the potential and that many local extrema exist. Rather than making extensive runs starting from a variety of potentials, we chose to use the more constrained subset of  $\mathcal{P}$ -symmetric potentials (5) and found that, indeed, even with only 2-3 parameters, much higher values of  $\gamma_{int}$  could be obtained as shown in Fig. 1(b). This is reminiscent of the observation in [10] that these bounds could only be reached if a  $\mathcal{P}$ -symmetric starting point was used for the search; in this work, we not only enforce the symmetry of the starting point but at all times in the optimization.

For the upper bound, we found a two-parameter potential close to the apparent maximum but below the theoretical maximum [Fig. 1(b)(i)]. The shape is characterized by shallow outer slopes with a divot in the center; the ground state wave function is localized to the divot with the highly delocalized first excited state above the divot. It was found to be necessary to constrain the slope  $A_2 > 0.005$  since the method of calculating  $\gamma_{int}$  presented in section II fails for shallow slopes. To avoid the unphysical feature of delocalized higher excited states, a distant wall was added to construct a three-parameter potential [Fig. 1(b)(ii)]. Such a change is expected *a priori* from previous work[16] to make no significant difference to  $\gamma_{int}$  as it is far from the region where  $\psi_0$  and  $\psi_1$  are large. For this well-like potential, we performed a maximization, adjusting  $A_2$ ,  $x_1$ , and  $x_2$  while fixing the outer walls to have a large slope ( $A_3 = 100$ ). The best potential found possesses  $\gamma_{int} = 0.59707$ , and has  $A_2 = 0.005$  which is the shallowest slope allowed by the constraint. The eigenvectors of the Hessian, calculated for the subspace excluding  $A_2$ , are well aligned with the parameters: the most significant eigenvector corresponds to  $x_1$ , the outer boundary of the divot. The other eigenvector corresponds to  $x_2$ , the position of the outer walls; this would be expected to have relatively little influence on  $\gamma_{int}$  since it controls a feature where the ground state wavefunction is small. Fixing the outer slopes at  $A_3 = 100$  as above, we also attempted to optimize  $\gamma_{int}$  with  $A_2$  constrained to be negative. It was found that  $\gamma_{int}$  increased as the slope approached zero, until a point was reached where the calculations became numerically unstable due to the asymptotic properties of the Airy functions. The highest value of  $\gamma_{int}$  which was found within a region of parameter space for which the calculation was still stable was  $\gamma_{int} = 0.5915$ , lower than the current maximum. We then performed similar optimizations on potentials with strict hard wall boundary conditions. The calculations for these potentials *were* numerically stable in all regions of parameter space which were explored: For  $A_2 > 0$ , a maximum of  $\gamma_{int} = 0.5959$  was found. For  $A_2 < 0$  a higher maximum of  $\gamma_{int} = 0.5968$  was found, though this is still lower than the current maximum of  $\gamma_{int} = 0.5971$ . Since a higher  $\gamma_{int}$  is found in potentials with  $A_2 < 0$  than for potentials with positive  $A_2$  in cases with strict hard wall boundary conditions, we speculate that a value

of  $\gamma_{int}$  higher than the current maximum found might be found for the finite  $A_3$  case. Nonetheless, we do not expect to see a significant improvement as the current maximum is already within  $\sim 0.5\%$  of the maximum value found in previous studies.

For the lower bound, a potential with the best value of  $\gamma_{int} = -0.1500$  was found using only two parameters [Fig. 2(b)]. This potential is characterized by steep outer walls and a “bump” in the middle: the ground state and first excited state wavefunctions cover the same spatial extent, but the bump causes the ground state to become spread out and relatively flat. Eigenanalysis of the Hessian of  $\gamma_{int}$  about this solution shows that one eigenvalue is significantly larger than the other, indicating that only one of the parameters is physically relevant. Moreover, the eigenvectors of the Hessian for this potential are aligned with the parameter space chosen to represent the potential. The higher eigenvalue is associated with an eigenvector along the  $x_1$  direction, which determines the position of the outer walls; the smaller eigenvalue is associated with the parameter that controls the slope of the outer walls. Because  $\gamma_{int}$  is invariant under rescalings of the form (15), a potential with identical  $\gamma_{int}$  can be constructed for a well of arbitrary width by tuning the slope of the bump.

The two parameter  $\mathcal{P}$ -symmetric potentials identified as the satisfying the apparent lower bound can be equivalently represented by a five parameter arbitrary potential. Optimization of the five parameter potential indeed finds this potential as the apparent global maximum. There are therefore no directions in this new parameter space which lead to a higher  $\gamma_{int}$ , despite relaxing the requirement that  $x_{-n} = -x_n$  and  $A_{-n} = -A_n$ . While the existence of asymmetric potentials with more negative  $\gamma_{int}$  cannot be ruled out, our analysis confirms that a  $\mathcal{P}$ -symmetric potential satisfies the apparent lower bound. We repeated this procedure for the upper bound using the two parameter  $\mathcal{P}$ -symmetric potential displayed in Fig. 2(b) as the starting point for optimization. It was found that despite relaxing the symmetry constraint no further improvement could be made so that the potential of Fig. 2(b) is also a local optimum with respect to the expanded parameter space. Analysis of the hessian was also performed on both of these five parameter optima. The eigenvalues and associated eigenvectors, shown in Fig. 3, reveal that for both upper and lower bounds the variation in the potential associated with the largest eigenvalue is indeed asymmetric.

The fact that we are able to achieve optimized  $\gamma_{int}$  within 1% of previous limits with far fewer parameters than in other representations of the potential[10], and also fewer parameters than required to numerically optimize  $\beta_{int}$ , is surprising since the calculated expressions for  $\gamma_{int}$  are far more complicated than those for  $\beta_{int}$ . Since the dimensionality of this parameter space is so small, it is instructive to visualize it directly: For our two-parameter optimizations, the value of  $\gamma_{int}$  is plotted over a portion of the parameter space [Fig. 4(a) and

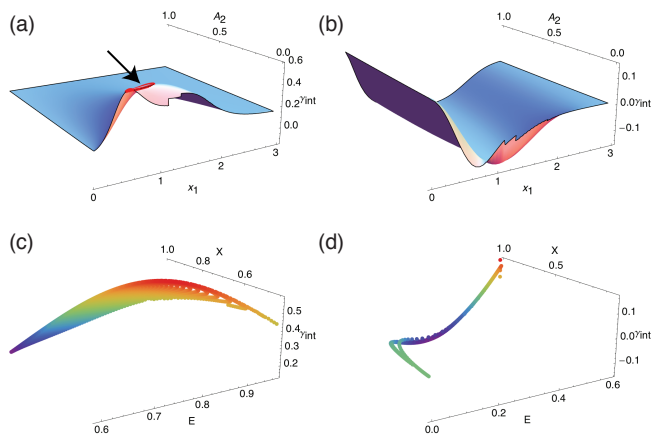


Figure 4: Visualization of the variation of  $\gamma_{int}$  as a function of the parameters  $x_1$  and  $A_2$  of a two-parameter  $\mathcal{P}$ -symmetric potential for the (a) upper bound and (b) lower bound. The region of parameter space where  $\gamma_{int}$  is within 2% of the maximum value is highlighted in (a) and indicated by an arrow.  $\gamma_{int}$  is also shown in the  $(E, X)$  parameter space for the (c) upper bound and (d) lower bound.

(b)]. The plot for the lower bound merely illustrates the results obtained from analysis of the Hessian, i.e. that the minimum is strongly curved about the optimal value of  $x_1$  but shallow with respect to  $A_2$ . The plot for the upper bound is more interesting: the region of parameter space for which  $\gamma_{int}$  is within 2% of the maximum value obtained is highlighted showing a clear ridge.

By calculating values of  $X = x_{01}/x_{01}^{max}$  and  $E = E_{01}/E_{02}$ , the natural parameters of the three-level ansatz[3], as a function of  $(A_2, x_1)$ , we are able to display  $\gamma_{int}$  re-parametrized in  $(E, X)$  space [Fig. 4(c) and (d)]. Here,  $x_{01}^{max} = 1/\sqrt{2E_{10}}$  in our units. Notice that the entire region explored in the numerical parametrization  $(A_2, x_1)$  collapses onto a narrow, elongated region in  $(E, X)$  space for the upper bound [Fig. 4(c)] and a complicated curved line for the lower bound [Fig. 4(d)]. These plots confirm the results of eigenanalysis of the Hessian: that essentially only a single parameter (or 2 for the upper bound) characterizes optimal  $\gamma_{int}$ .

The results of the three-parameter optimization and the plot in fig. (4) both suggests that the truly optimal  $\mathcal{P}$ -symmetric potential for the upper bound has shallow outer slopes  $A_2 \rightarrow 0$ . Such a potential can be transformed, using (15), to a potential of equivalent  $\gamma_{int}$  but where the outer slope is unity and the central well is far narrower and sharper. Since the central divot for the transformed potential resembles a Dirac delta function, we studied the second hyperpolarizability of the family of potentials

$$V(x) = |x| - \alpha\delta(x) \quad (17)$$

where  $\alpha$  is the single adjustable parameter. Values of  $\gamma_{int}$  as a function of  $\alpha$  are displayed in fig. 5 and the maximum value is found to be  $\gamma_{int} = 0.58194$  which occurs

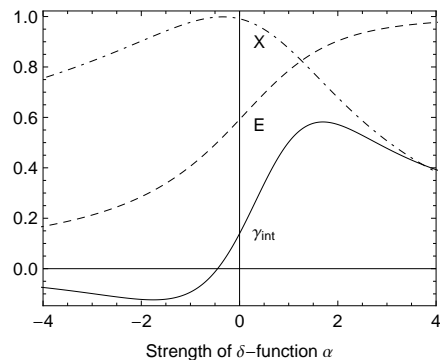


Figure 5: Plot of  $\gamma_{int}$ ,  $E = E_{10}/E_{20}$  and  $X = x_{10}/x_{10}^{max}$  as a function of  $\alpha$  for the for the potential  $V = |x| - \alpha\delta(x)$ .

when  $\alpha = 1.69552$ . Despite the simplicity of this one-parameter potential, the result is only 3% smaller than the best reported so far and only fractionally smaller than those found with the two and three parameter potentials above.

We now turn to the question of whether the simple, but optimal or nearly so, potentials that were identified above resemble either those previously found [10] or possess the universal features identified in [13]. Comparing our best optimized potentials and wavefunctions to those in [10], some qualitative similarities are apparent. For the upper bound, the potentials in Watkins *et al.* are roughly symmetric near their lowest point. They feature a central divot within a wider well where the ground state wave function is localized within the central divot and the first excited wave function is relatively delocalized compared to the ground state. For the lower bound, the potentials feature a steep well within which both the ground state and first excited state are localized, and a central bump which causes the ground state to be spread out within the well. These qualitative features are shared by the potentials obtained in this work, but many extraneous details are removed by the highly constrained, judiciously chosen representation.

In table II we display values of  $X$  and  $E$ , together with the values of these parameters that extremize  $\gamma_{int}$  for the three-level ansatz[3] and those possessed by the best previously found potentials[10]. Values are also shown for two elementary potentials, the triangle well and infinite square well. The results for the upper bound are quite consistent with those of Watkins *et al.* if the breadth in the range of these values identified by the Monte Carlo study[13] is taken into account. The values of  $E$  and  $X$  are also displayed in Fig. 5 as a function of  $\alpha$ , the strength of the  $\delta$  function, in the potential (17);  $E$  is a monotonically increasing function of  $\alpha$  while  $X$  is a monotonically decreasing function. Crudely, these explain the existence of a maximum  $\gamma_{int}$  as representing the trade-off between increasing the motion of the electron (associated with high  $X$ ) versus enhancing transitions to other states (associated with low  $E$ ).

Bound	Potential	$\gamma_{int}$	$E$	$X$
Upper	3-level ansatz[3]	1	0	0
	Best from [10]	0.5993	0.5767	0.5150
	Arb. 5 param.	0.43601	0.5765	0.6512
	$\mathcal{P}$ 3 param.	0.59707	0.8665	0.7468
	$ x  - \alpha\delta$	0.58194	0.6842	0.7385
	Triangle well $ x $	0.1392	0.5918	0.9911
Lower	3-level ansatz[3]	-0.25	0	$\pm 1$
	Best from[10]	-0.1500	0.1493	0.6658
	$\mathcal{P}$ 2 param.	-0.1500	0.2855	0.9416
	$ x  - \alpha\delta$	-0.1236	0.2438	0.9222
	Infinite square well	-0.1262	0.3750	0.9801

Table II: Second hyperpolarizabilities and physical parameters  $X = x_{01}/x_{01}^{\max}$  and  $E = E_{01}/E_{02}$  for the optimized potentials obtained in this work.

#### IV. CONCLUSION

We have optimized the intrinsic second hyperpolarizability  $\gamma_{int}$  of a piecewise linear potential well with respect to parameters that control the shape of the potential. We found solutions that lie within the range  $-0.15 \leq \gamma_{int} \lesssim 0.60$  in agreement with the apparent bounds established in previous numerical optimizations[10]; these both fall short of the Kuzyk limits[3]. By using two types of potential, one where all slopes were allowed to vary and another with explicitly enforced symmetry, we demonstrated that  $\mathcal{P}$ -symmetric potentials satisfy the apparent lower bound for  $\gamma_{int}$  and come within  $\sim 0.5\%$  of the apparent upper bound. The parametrization used constrains the potential to be smooth, preventing the occurrence of rapid oscillations which do not affect  $\gamma_{int}$  [16]. Because of this and the strong symmetry constraint, the optimal  $\mathcal{P}$ -symmetric potentials found were characterized by only 2 – 3 parameters. Of these, a *posteriori* analysis of the Hessian revealed that effectively only one or two, for the lower and upper bound respectively, were important

These results are reminiscent of those obtained earlier for  $\beta_{int}$ [14], yet the number of parameters required to optimize  $\gamma_{int}$  appears to be smaller even though it is a more complex object, containing more terms and involving higher derivatives. At least part of the reason for this is that for  $\gamma_{int}$  there exists a “compatible” symmetry operator,  $\mathcal{P}$ , which can be used to constrain the

shape of the potentials; this was not possible for  $\beta_{int}$  where  $\mathcal{P}$ -symmetric potentials automatically have  $\beta = 0$ . However, even though we have shown that  $\mathcal{P}$ -symmetric potentials can have optimal or near-optimal second hyperpolarizabilities, it is not clear whether the apparent upper bound  $\gamma_{int} \sim 0.6$  achieved by Watkins and Kuzyk can be achieved with a  $\mathcal{P}$ -symmetric potential or whether a small amount of asymmetry is necessary. Moreover, the reason why local potentials fall short of the Kuzyk bounds remains opaque.

The small parameter space allows us to propose a clear design paradigm for new chromophores, within the limitations of the model one-electron 1D system studied. Neglected here, for example, are multi-electron interactions, molecular ordering and inter-molecular electron hopping. Nonetheless, the potentials obtained could be realized, for example, by a centrosymmetric molecule with a central attractive or repulsive group—for positive or negative  $\gamma_{int}$  respectively. The strength/electronegativity of the central group and the ratio of the length of the central and peripheral groups can then be tuned to give high  $\gamma_{int}$ . Unfortunately, most practical chromophores are  $\pi$  conjugated systems in which there are approximately as many electrons as there are sites on the molecule, thus the consequences for them from this single electron calculation are clearly very speculative. Nevertheless, homologous sequences already studied for high  $\gamma$  as a function of chain length, e.g. [6] could likely be enhanced by including such a central group with different electronegativity. Any other means of achieving a potential well or inducing a significant phase shift in wavefunctions passing through the center of the molecule is also likely, even in multi-electron systems, to offer a route for achieving larger  $\gamma_{int}$ . The present analysis provides other important insights: first, that since the “true” parameter space for  $\gamma_{int}$  is so small, only rough tuning of the molecular design ought to be necessary. Secondly, this work again confirms that there are a large set of modifications to optimized potentials, e.g. rapid oscillations, that will not change  $\gamma_{int}$  and need not be considered in planning what molecules to synthesize. As has been previously noted, materials with high  $\gamma_{int}$  could also be realized more directly in other ways, such as through composite materials.

- 
- [1] R. W. Boyd, *Nonlinear Optics, 3rd ed.* (Academic Press, 2008).
- [2] Y. R. Shen, *The Principles of Nonlinear Optics* (John Wiley & Sons, 2003).
- [3] M. Kuzyk, Phys. Rev. Lett. **85**, 1218 (2000).
- [4] M. Fujiwara, K. Yamauchi, M. Sugisaki, K. Yanagi, A. Gall, B. Robert, R. Cogdell, and H. Hashimoto, Phys. Rev. B **78**, 161101 (2008).
- [5] J. M. Hales, J. Matichak, S. Barlow, S. Ohira, K. Yesudas, J.-L. Bredas, J. W. Perry, and S. R. Marder, Science **327**, 1485 (2010).
- [6] T. Luu, E. Elliott, A. Slepkov, S. Eisler, R. McDonald, F. Hegmann, and R. Tykwinski, Organic letters **7**, 51 (2005).
- [7] J. C. May, I. Biaggio, F. Bures, and F. Diederich, Applied Physics Letters **90**, 251106 (2007).
- [8] B. Champagne and B. Kirtman, Physical Review Letters **95**, 109401 (2005).

- [9] B. Champagne and B. Kirtman, *Journal of Chemical Physics* **125**, 024101 (2006).
- [10] D. Watkins and M. Kuzyk, *JOSA B* **29**, 1661 (2012).
- [11] K. Tripathy, J. Moreno, M. Kuzyk, B. Coe, K. Clays, and A. Kelley, *The Journal of chemical physics* **121**, 7932 (2004).
- [12] J. Zhou, U. Szafruga, D. Watkins, and M. Kuzyk, *Phys. Rev. A* **76**, 053831 (2007).
- [13] S. Shafei, M. Kuzyk, and M. Kuzyk, *JOSA B* **27**, 1849 (2010).
- [14] T. J. Atherton, J. Lesnfsky, G. A. Wiggers, and R. G. Petschek, *Journal of the Optical Society of America B* pp. 1–8 (2012).
- [15] M. Kuzyk and C. Dirk, *Phys. Rev. A* **41**, 5098 (1990).
- [16] G. Wiggers and R. Petschek, *Optics letters* **32**, 942 (2007).